Pergamon

Available online at www.sciencedirect.com
SCIENCE DIRECT®

Cement and Concrete Research 33 (2003) 1331–1345

CEMENT AND CONCRETE RESEARCH

The macro- and micro properties of cement pastes with silica-rich materials cured by wet-mixed steaming injection

D.S. Wu[a,*], Y.N. Peng[b]

[a]Department of Architectural Engineering, Chung-Kuo Institute of Technology, No. 56, Sec. 3, Hsing Lung Road, Taipei 116, Taiwan, ROC
[b]Department of Civil Engineering, National Chiao-Tung University, Hsinchu, Taiwan, ROC

Received 23 January 2001; accepted 5 February 2003

Abstract

This research used cement pastes with a low water/blaine ratio (W/b = 0.27). Rice husk ashes (RHA) burned at 700 and 850 °C, silica fume, silica sand (Ottawa standard sand), etc., were the added ingredients. Wet-mixed steam injection (WMSI) was at five different temperatures: 65, 80, 120, 150 and 180 °C. We investigated cement pastes with added silica-rich materials. For different WMSI temperatures and times, we explored the relations between compressive strength, hydration products, and pozzolanic reaction mechanism. From scanning electron microscopy (SEM) and EDS, we know that hydration products become very complicated, depending on the WMSI temperatures and times. It is difficult to determine the direct effects on the strength based on changes in the products. Experimental results, however, clearly showed that the compressive strength was worst for 80 °C and best for 180 °C. High-temperature WMSI is best with 4-h presteaming period and 8-h retention time. Curing in saturated limewater for 28 days did not increase the strength. The three types of silica-rich materials used in this research all participated in the reaction during high-temperature WMSI; they helped to increase the strength. Addition of Ottawa standard sand resulted in the best strength, followed by addition of RHA, while addition of silica fume was worse than the others. Specimens treated with high-temperature WMSI would swell slightly if they were placed in air. This was different from normal-temperature curing.

Keywords: Curing; Hydration; Microstructure; Shrinkage

1. Introduction

Low-temperature wet-mixed steam injection (WMSI) has been used in precast concrete for several years. By hot water curing or steaming curing, a 95% hydration rate can be achieved in a few hours [1,2]. However, this concrete easily cracks due to the temperature difference between the inside and the outside. The concrete shows high compressive strength in early stages and weaker strength in late stages than those cured at normal temperatures [3]. Recently, the effects of temperature and retention time on steaming curing process and the reaction mechanism of type I cement with single Portland materials, e.g., slag, fly ash and silica fume, have been well studied [4–11]. However, few studies have investigated the reaction mechanism of steam-injected cement with silica-rich materials, e.g., rice husk ash (RHA), silica fume and silica sand. Due to large quantities of SiO_2 in RHA and silica fume, the hydration products CH can produce more CSH gels in pozzolanic reaction at normal temperatures. This leads to a structure of paste or concrete, to which adequate amounts of RHA and silica fume are added, having high early compressive strength characteristics. The final compressive strength and durability are worse than those without Portland cement substitute materials [12,13]. Several documents indicated that silica can be involved in hydration reaction at high temperatures [4,7,14]. By adding silica-rich materials and using steam curing, concrete compressive strength may be improved. These principles show that the use of silica-rich materials to improve final concrete compressive strengths is a feasible strategy.

2. Test program

2.1. Materials and specimen preparation for steaming

An overview of the test program is shown in Fig. 1. Type I Portland cement with a fineness of 3500 cm^2/g and silica-

* Corresponding author. Tel.: +886-2-29346863; fax: +886-2-29353447.
E-mail address: dswu@mail.ckitc.edu.tw (D.S. Wu).

0008-8846/03/$ – see front matter © 2003 Elsevier Science Ltd. All rights reserved.
doi:10.1016/S0008-8846(03)00059-0

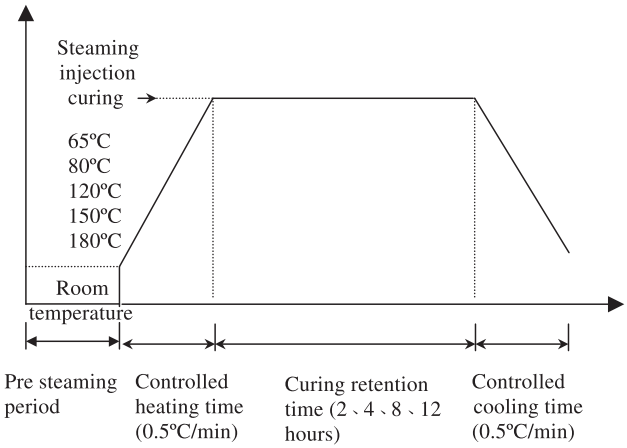

Fig. 1. Process for WMSI.

rich materials were the base materials. The RHA was made at two temperatures (700 and 850 °C), with finenesses of 3550 and 4100 cm^2/g and a specific gravity range of 1.86–2.18 (Table 1). The fineness of silica fume was 10,820 cm^2/g. Standard sand from Ottawa USA was used. The coarse one satisfied ASTM C109, with a relative weight of 2.67. The fine one satisfied ASTM C190. The ratio of superplasticizer/blaine (Sp/b) was 1.58%, which conformed to ASTM C494 G-type standard. In the microscopic experiment, the experimental variables were as follows (see Tables 2 and 3): CaO/SiO_2 was 1.8 mol ratio, as determined by the optimal results from compressive experiments with the RHA additive (see Fig. 2). Since it took time to solidify cement pastes, if steam curing was applied to unsolidified samples, water in the samples may boil. This led to sample swelling and cracks, further affecting the structure of concrete. Therefore, all WMSI groups in this experiment were based on the experimental results in Fig. 2. All mixtures settled for 4 h before undergoing WMSI.

The structure of steam-cured product was investigated using macro- and microanalysis. From a macroscopic viewpoint, the characteristics of shrinkage and compressive strength were evaluated. For microanalysis, nuclear magnetic resonance (NMR), scanning electron microscopy (SEM), EDS, TGA, etc., were used to examine the hydration mechanisms and analyze the hydration products. The evaluations included the differences in cement hydration products due to various CaO/SiO_2 ratios with various silica-rich materials added, the effects of curing temperature and catalysis time on pozzolanic reaction, and the relationship between the degree of hydration and the compressive strength.

Table 1
Chemical elements of silica-enriched Portland materials

Elements (oxide)		Temperature			
		RHA 700 °C	RHA 850 °C	Silica fume	Ottawa standard sand
SiO_2		92.152	93.215	93.421	98.254
MgO		0.512	0.545	1.524	–
SO_3		0.794	0.707	0.151	–
CaO		1.597	1.378	1.380	–
K_2O		3.973	2.927	2.187	–
Na_2O		0.993	0.878	0.101	–
Fe_2O_3		0	0.356	1.344	–
Specific gravity	3550	1.86	1.98	–	–
	4100	2.09	2.18	2.26	–

Table 2
Experimental variables

Items	Variables
Ignition temperature of RHA (°C)	(A) 700 (B) 850
Size of RHA (cm^2/g)	(A) 700 or 850 °C 200 = 3550 (B) 700 or 850 °C 200S = 4100
Silica fume (cm^2/g)	10,820
Ottawa standard sand	(A) ASTM C109 (B) ASTM C190
RHA/cement (CaO/SiO_2 ratio after mixing)	See Table 3
W/b	0.27
Sp/b (%)	1.58
Steaming injection curing (see Fig. 1) (°C)	(A) Low temperature: 65 and 80 (B) High temperature: 120, 150 and 180
Room temperature curing (25 °C)	Curing in the saturated lime water
Ages	(A) Room temperature curing: 1, 3, 7, 28, 56 and 90 (days) (B) Steaming injection tests: 1, 3, 7, 28, 56, 90, 180 and 360 (days)

2.2. Steam hydration testing

The main test apparatus for steam hydration was an integrated steam generator and chamber system. It was composed of a steam generator, an autoclave, water softness machinery and multiple temperature control settings with a safety defuse temperature of 200 °C (Fig. 2). Following the ASTM C490 methods, a longitudinal sample with a size of $2.54 \times 2.54 \times 25.4$ cm was prepared. After 28 days, the samples were cured in a constant temperature (25 °C) and humidity chamber, and the degree of shrinkage was measured on days 28, 56, 90, 120 and 180. For compressive strength test, a specimen with a size of $5 \times 5 \times 5$ cm was used. The detail test conditions can be seen in the ASTM C39 methods.

Table 3
Ratio of calcium and silica in a mixture of RHA and cement

Number	Amount of cement	Amount of RHA	700 °C RHA CaO/SiO_2 ratio	850 °C RHA CaO/SiO_2 ratio
1	100	0	3.2153	3.2153
2	85	15	1.8249	1.7938
3	80	20	1.5479	1.5162
4	67	33	–	1.0066
5	50	50	–	0.5957

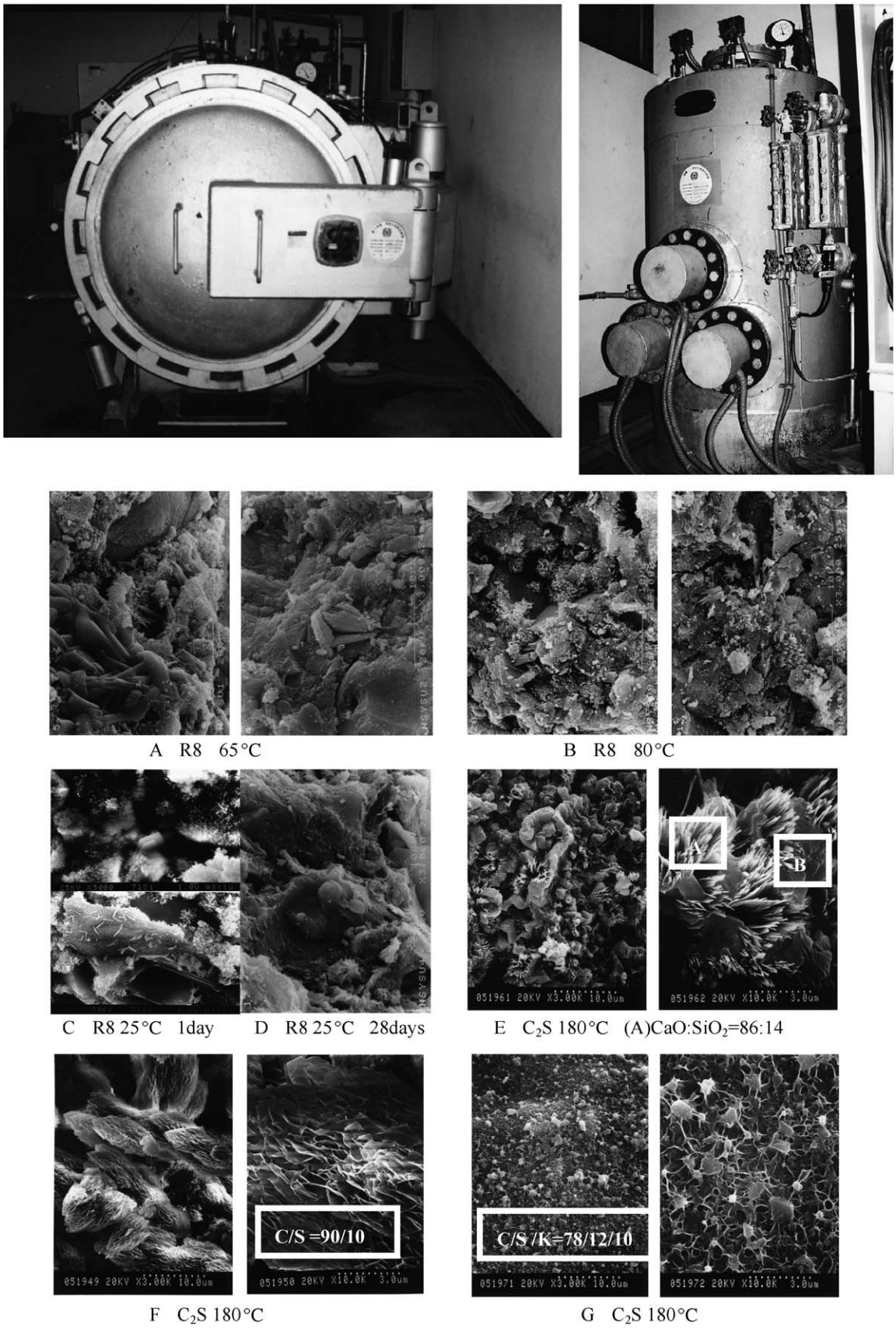

Fig. 2. Steam generator for WMSI and autoclave.

2.3. Techniques for characterizing microhydrates

The techniques used for characterizing the microhydrates are shown in Table 4. The specimen used for the compressive test was used for microanalysis. Hydration of specimen was terminated by methanol; then, the specimen was vacuumed and ground to pass the no. 325 sieve. For the NMR test, the ground powder was placed in a spectroscopic magnet. ^{29}Si, used as a nucleus, and tetramethylsilica, used as a base material, emitted electromagnetic waves and produced a NMR spectrum. The peak area in the nuclear magnetic spectrum is related to the degree of hydration, the pozzolanic reaction and the bond lengths of Si-Si in CSH gel. For X-ray analysis, the ground dust was further pressed into a $2.5 \times 1.4 \times 0.1$ cm specimen for qualitative analysis of hydration products. For the TGA test, again, the specimen used for the compressive test was used, and the hydration of the specimen was terminated by methanol. Then, the specimen was vacuumed and ground to pass the no. 325 sieve. The ground powder was heated at a rate of 20 °C/min. Then, the TGA spectrum was plotted on a multiple-stage plotter. The results identified the degree of hydration and $Ca(OH)_2$. For measuring the quantity of combination water, the specimen was chopped into small pieces. Fragments with a size between sieve nos. 16 and 30 were used. The selected fragments were baked in an oven at 105 °C for 24 h and then weighed. The weight is denoted as W_1. Afterward, the sample was placed in an 800 °C oven for 15 min. It was cooled down to 50 °C and weighed again. The second weight is denoted as W_2. The quantity of combination water (%) can be calculated as $(W_1 - W_2)/W_1 \times 100\%$. On SEM, the sample at each storage stage was observed. The hydration of the sample was terminated by methanol; then, the sample was electroplated with gold for analysis on an SEM. Also, the EDS was used to detect elements.

3. Test results and analyses

3.1. Effect of curing temperatures on hydration products

The hydration of cement includes hydrolysis and combination with water. In the steaming process, the duration of each period (such as presteaming period, controlled heating time, curing retention time and controlled cooling time) affects the creation of the hydration products and the compressive strength. Initially, in the experiments, we used 180 °C steaming temperature and added different amounts of RHA to find out the optimal steaming time and retention time. The experimental results show that it was best to have 4-h retention time and 8-h steaming time with the amount of additive $CaO/SiO_2 > 1.8$, as shown in Fig. 2.

In this study, cement paste with a low gel content was retained for 4 h after mixing before it was steamed. The initial stage of hydration (the dissolving stage) was the same as others. After 4 h of retention, heat was released as the paste was transforming into gel. In addition, heat was provided by steam from the steamer. This definitely accelerated the transformation of gel into crystals. This is different from the normal-temperature process in which paste becomes hydration products. According to literature, hydration products in cement created at temperatures below 100 °C have no large variations in their physical properties [6,15]. According to Refs. [6,14], typical high-temperature curing creates mainly the following crystals: 11 Å tobermorite ($C_6S_2H_3$), α-C_2SH, xonotlite, and gyrolite.

In this study, we found that many types of hydration products were created at different steaming temperatures. They are much more complicated than those created in normal-temperature curing. At temperatures below 100 °C, the properties of the hydration products created at 65 and at 80 °C are different. To compare these products, we steam

Table 4
NMR test results and compressive strengths of cement pastes at different WMSI temperatures

Temperature (°C)		180	150	120	80	65	Room (25 °C) age (28 days)
Cement + Sp + RHA	α (%)	86	75	78	69	76	79
	Psi	4.75	4.38	4.41	3.05	4.12	3.29
	Compressive strength (MPa)	113.4	107.1	100.9	79.3	83.3	94.3
C_3S + Sp + RHA	α (%)	91	84	80	76	71	–
	Psi	5.00	4.95	4.72	2.92	3.15	–
C_2S + Sp+ RHA	α (%)	58	59	58	58	56	–
	Psi	4.73	4.22	4.07	3.52	3.83	–
Cement + Sp	α (%)	84	78	76	68	75	77
	Psi	4.69	4.64	4.35	3.20	4.13	3.23
	Compressive strength (MPa)	99.6	89.7	82.7	72.3	74.5	80.7
C_3S + Sp	α (%)	89	88	70	66	66	–
	Psi	6.08	5.12	4.67	2.82	3.31	–
C_2S + Sp	α (%)	46	48	45	47	45	–
	Psi	4.40	4.28	4.12	3.69	4.00	–

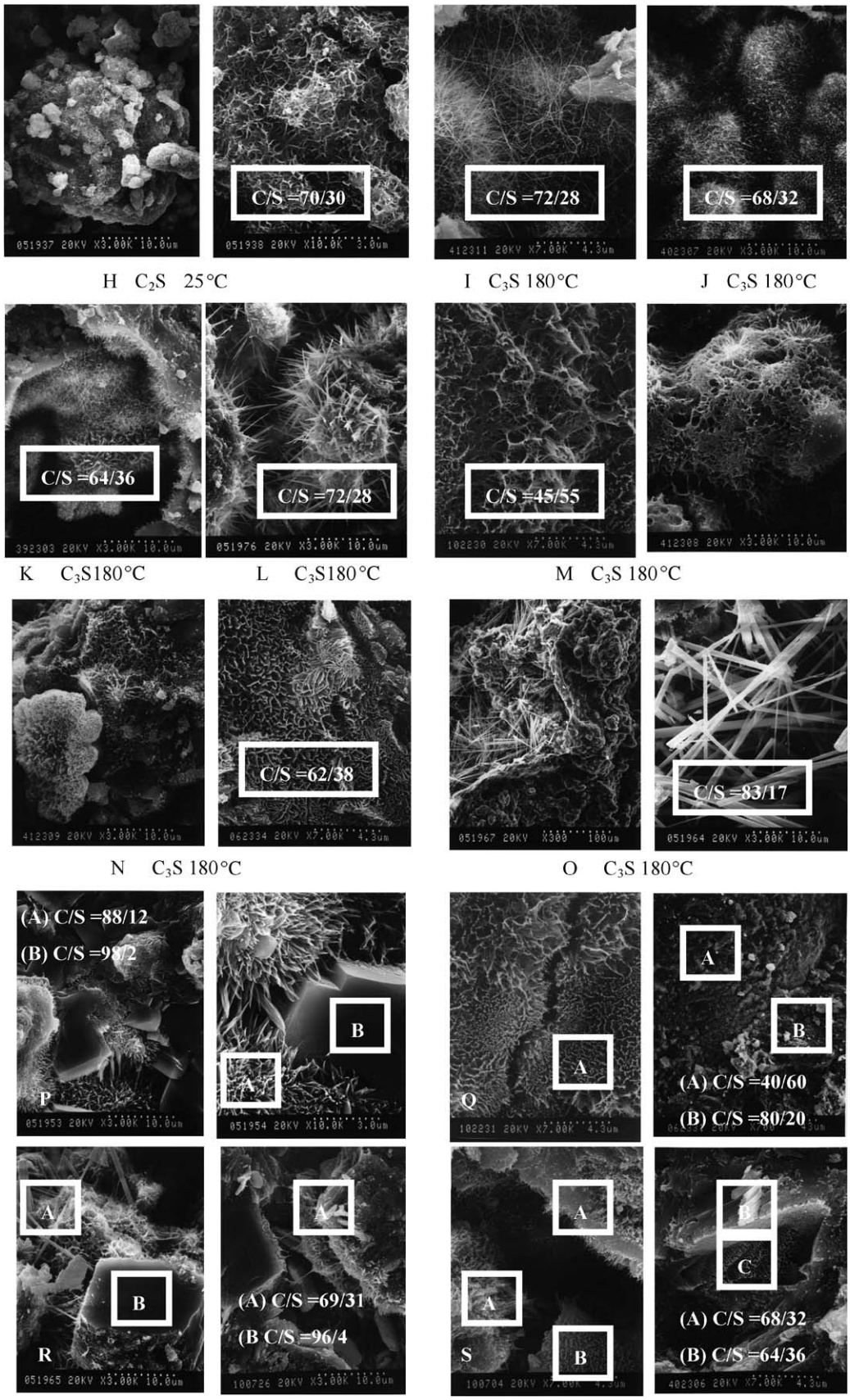

Fig. 3. SEM observation of C_3S, C_2S and steam-induced hydrates in cement pastes with RHA.

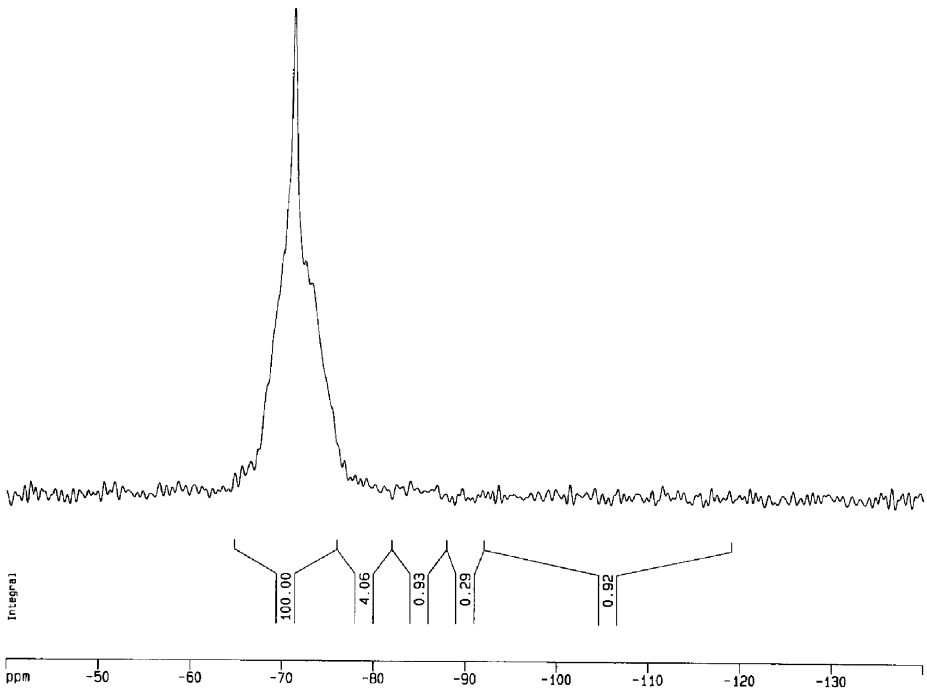

Standard

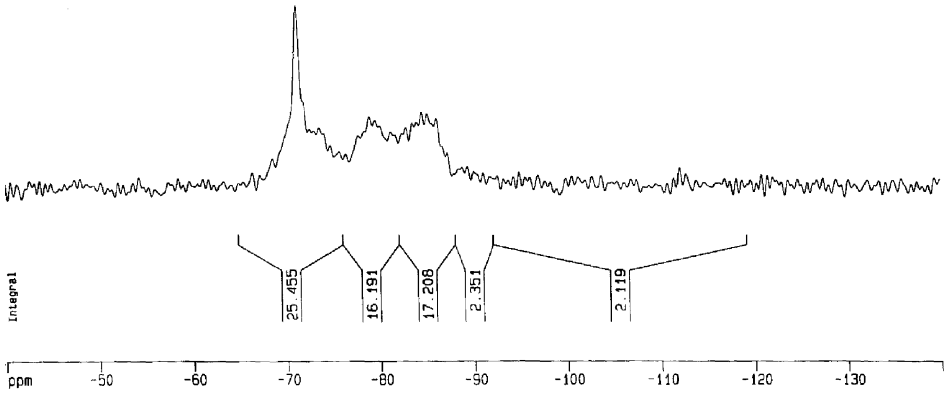

65 °C

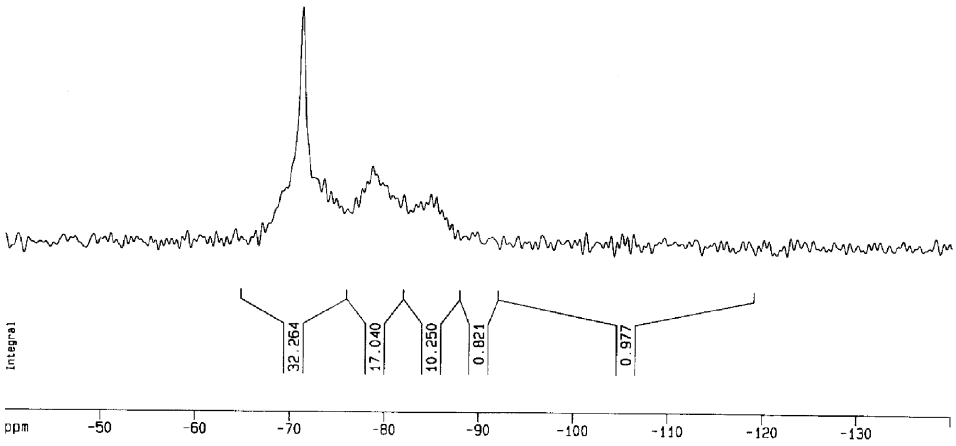

80 °C

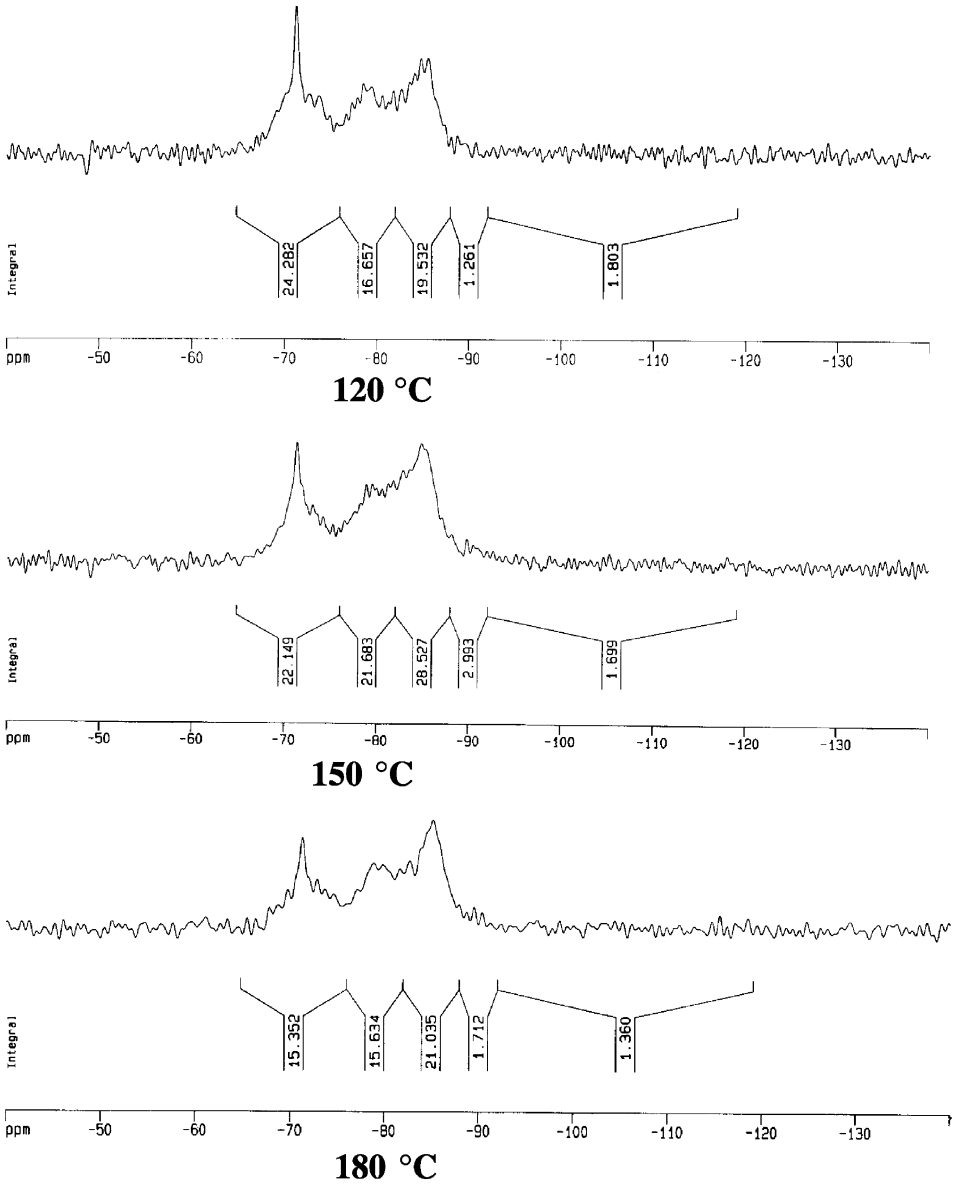

Fig. 4. ^{29}Si NMR test data for hydrates in wet-mixed specimens steamed at different temperatures.

tested four types of minerals: C_3S, C_2S, C_3A and C_4AF. We used SEM for observation and EDS for analysis. In the SEM experiment, we used crushed specimens for observation. The broken surfaces we observed must have been from the weak spots of the specimens. The hydration products and structure of those spots must be important indicators of strength. Since there are so many products, we describe only the hydration products from two minerals, C_2S and C_3S, which have great effects on strength, as described in the following subsections.

3.1.1. Steam curing at lower temperatures (65 and 80 °C)

Experimental results showed that cement pastes with different silica-rich pozzolanic materials and steamed at 65 °C had hydration products that were mainly CSH, CH, AFt and AFm. This was not much different than normal-temperature curing. From SEM observation, we found that the products of low-temperature curing were denser than those of 1-day, normal-temperature curing because of the influence of high temperatures. Compared to the 28-day, normal-temperature curing group, the steam curing group had looser structures and more microcracks. This was more obvious at 80 °C than 65 °C (see Fig. 3A and B). It may be that there was more quasi-stable CSH(A) generated at 80 °C. This quasi-stable product could expand during the formation of crystals, creating a pressure that forced the microcracks to expand and making it more difficult for the quasi-stable CSH products to transform into stable CSH. This may be the main reason that 80 °C was inferior to 65 °C.

The NMR experiments prove that (see Table 4 and Fig. 4) the degree of hydration and the lengths of silica bonds are better at 65 °C than at 80 °C. The products of 1-day, normal-temperature curing are mainly spiky CSH gels made of imperfect crystals. The amount of CH and pores are also greater than those of the steam curing group (see Fig. 3A–D). This is the main reason that the 65–80 °C steam curing group is stronger than the 1-day, normal-curing one but weaker than those older than 28 days. Experiments showed that 80 °C curing was obviously inferior to 65 °C curing both in quality and in strength. If low-temperature curing is used at construction sites, the curing temperature should be strictly set at less than 65 °C and the curing retention time should be less than 8 h.

3.1.2. Steam curing at higher temperatures

3.1.2.1. Steam curing products from C_2S. Since water was used (water/blaine ratio (W/b) = 0.27) in this study, the hydration of cement can still be achieved even with no further supply of steam. Products from steam curing C_2S with silica-rich materials are layered and have more than three types (Fig. 3E–G). These are quite different from those dry-mixed steam cured. The thicknesses of the layers are about 0.1 μm. Spikes are formed between pores, especially in slits between CH. The ratio of CaO/SiO_2 = 86:14 was found in the sample by an EDS analysis. The ratio is higher in the samples than in C_2S for which the ratio of CaO/SiO_2 is 79:21. When pores are filled with these hydration products, this could compensate for the strength lost due to cracks in CH. Fig. 3F shows the surfaces of typical products in steam curing. Another type also often grows on the surface of C_2SH(A). The ratio for $CaO/SiO_2/K_2O$ is 78:12:10 (see Fig. 3G). However, the degree of hydration is more complete in steam curing, and the ratio of CaO/SiO_2 is 70:30 in this type (see Fig. 3H).

3.1.2.2. Steam curing products from C_3S. Products from C_3S steam curing have more than eight types. Type I (see Fig. 3I–L) grows from the surface of C_3S then further grows to the surrounding pores or cracks. When this type was first produced, it was similar to products (CSH) from normal-temperature curing. However, little CH was found inside. This was due to the loss of free water in pores in stream curing. Not enough water reacted with CaO to form CH. Some filament-like products could grow up to a size of 20 μm. Generally, the diameter is below 0.1 μm, and the ratio of CaO/SiO_2 is 72:28 (see Fig. 3I). The length difference is probably due to different concentrations caused by different curing temperatures and ionization. The CSH shown in Fig. 3J is similar to that of normal curing temperatures with CaO/SiO_2 ratio of 68:32. Coarse and fine products simultaneously exist in pores (see Fig. 3K). The CaO/SiO_2 ratio for coarse ones is 64:36. Although three types of products (see Fig. 3I–K) show significant difference, the CaO/SiO_2 ratio decreases as the magnitude of the product increases. This implies that certain relationships exist between these three types of products. Higher CaO/SiO_2 ratio was found due to the lower W/b ratio used in this study in comparison with that in the literature. Therefore, this led to a higher CaO/SiO_2 ratio in the same volume. Type II products have thin layers with triangular spikes. The ratio of CaO/SiO_2 is 72:28. This pattern is the same as that shown in Fig. 3I. More space is found between spikes. In theory, the strength is not as high as that of type I. The strength of the three-dimensional structure created from connecting two-dimensional layers is unknown. The structure of type III (see Fig. 3M) products is one of layers of net superimposed. The ratio of CaO/SiO_2 is 46:54. The amount of SiO_2 is more than that of CaO. It implies that when more SiO_2 are involved in the formation of products, these dense net-like products could transform large holes into disconnected small holes. This helps to inhibit potential change, drying and shrinking and enhance strength. Type IV (see Fig. 3N) is one of the products formed on the surface of C_3S. The ratio of CaO/SiO_2 is 62:38. The patterns shown in Fig. 3K, Q and N are very similar. They show differently under an SEM. It implies that they are silica-rich layered products. The pattern of type V is needle-shaped products. It can be generated from any fissures in the products. The length of the sticks can be over 50 μm. They are the longest products and do not grow in the same direction. Although the cross sections of the stick-like products are different, the cross section and scale are the same from the top to the bottom of the same stick. The ratio of CaO/SiO_2 is 83:17. This ratio is the same as that of C_3S without hydration. The ratio of CaO/SiO_2 in type VI (see Fig. 3P) is very close to that of C_3S without hydration. This may come from the pozzolanic reaction of CH and SiO_2. Therefore, the CaO/SiO_2 ratio is higher. The amount of SiO_2 increases with the reaction time, and the pattern of this product may be transformed into the shape shown in Fig. 3R. The CaO/SiO_2 ratio in type VII (see Fig. 3Q) is 40:60. This is the only product with more SiO_2 than CaO. (The other is type III.) This often exists on the surface of silica sand and RHA. Especially for silica sand, this type of product can be found on almost every grain of sand. This is due to the even distribution and continuity of SiO_2. This characteristic can cause to water diffuse into samples and increase the degree of hydration. This mechanism can be applied in dry mixture models and improve the steam curing process. Fig. 3R shows type VIII products. With a CaO/SiO_2 ratio of 69:31, area A in Fig. 3R is CH, while area A shows CH products from pozzolanic reaction. Some stick-like products (like Fig. 3O) can also grow. If this further grows, CaO would be gradually replaced by SiO_2. This looks like areas A–C in Fig. 3S. When the generated products on the CH surface connect together, the pore becomes smaller. The cracks are also filled with crisscrossed and dense products. This can enhance strength.

3.2. Effects of curing temperature, degree of hydration and bond lengths of Si-Si in CSH gel on compressive strength

This research used the principles of NMR (^{29}Si NMR) to obtain the degree of hydration and the bond lengths of Si-Si in CSH gel of the products generated at different times for different fineness and amounts of additives [17], i.e.,

$$\alpha = (1 - I(Q^0)/I^0(Q^0)) \times 100\% \quad (1)$$

where Q^0, Q^1 and Q^2 denote the degree of binding of the SiO_4 quadrilateral. The superscripts 0, 1 and 2 denote the shared atomic numbers of SiO_4 quadrilateral. $I(Q^0)$ and $I^0(Q^0)$ denote the integral intensities of the hydrated cement paste and material powder for the signal Q^0. The lengths of the silica ions of CSH gel (Psi) are defined as

$$\text{Psi} = 2[1 + I(Q^2)/I(Q^1)]. \quad (2)$$

Three base materials, which are cement, C_3S and C_2S, with or without RHA, were tested individually in the NMR experiment. However, since the unit prices of C_3S and C_2S were high, theses two materials were not used for compressive test. Results showed (Table 4) the degree of hydration, bond lengths of Si-Si in CSH gel and compressive strength at normal curing temperatures of 28 days were worse than those from steam curing at high temperatures. However, these results were the same as those steam cured at 80 °C and better than those steam cured at 65 °C. For the same material treated at high WMSI temperatures, the completeness, strength and degree of hydration increased with the steam curing temperature. The degree of hydration for RHA-added groups is better than those without the addition. The compressive strength is 20% stronger with normal-temperature curing of 28 days age and 20–32% stronger with steam curing. These results show that RHA has significant contribution to compressive strength for steam curing temperatures of 150 and 120 °C. The bond lengths of Si-Si in CSH gel do not increase with the steam curing temperature for RHA-added groups. However, the increase of bond lengths of Si-Si in CSH gel with the rise of steam temperatures was evident in the groups without additives. Compared with the cement group, the degree of hydration can reach 90% for C_3S at 180 °C steam curing temperature, while it is lower than 60% for C_2S and there are no significant differences (45–60%) at different steam curing temperatures. Unlike C_3S, the bond lengths of Si-Si in CSH gel is not proportional to the curing temperature of C_2S.

3.3. The effect of curing temperature on shrinkage

Pores in a cement paste occupy 40–55% of the volume. There are evaporable water, water adsorbed by gels and interlayer water in pores. These three kinds of water are different from chemical water bonded to hydration products. When the outside temperature is higher or the humidity is lower than the sample, the water in the pores evaporates to the outside. This leads to a volume decrease, further producing cracks or deformities [1]. Generally, shrinkage in concrete can be categorized into three groups [1,18]:

1. *Plastic shrinkage.* This is also called capillary shrinkage. Loss of water in capillary makes negative capillary pressure inside the sample. This can lead to paste shrinkage. Plastic shrinkage is often the reason for cracks on the surface of cement.
2. *Autogenous shrinkage.* CSH gel is one that the products of cement hydration can not completely fill, causing the formation of pores. If no more added water is provided, dryness in these pores can cause the self-desiccation phenomenon. This leads to autogenous shrinkage.

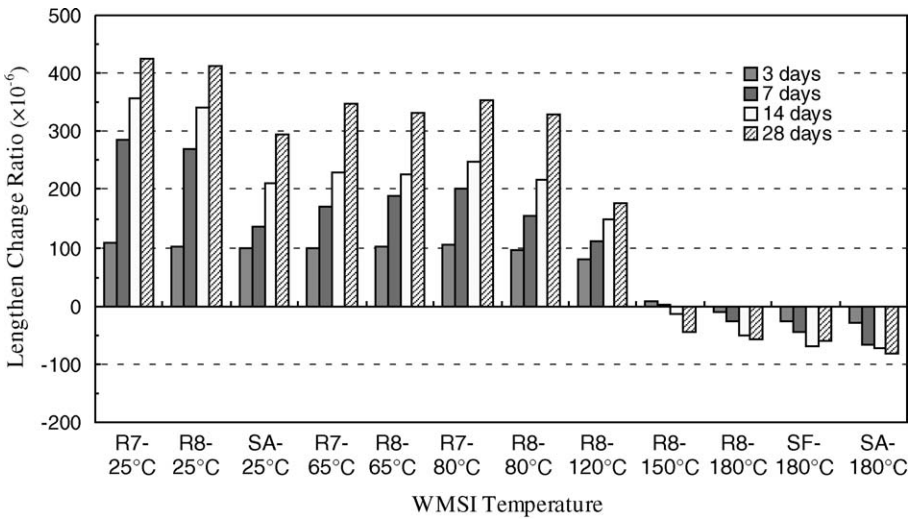

Fig. 5. Volume variations of wet-mixed specimens steamed at different temperatures.

3. *Dry shrinkage.* In a dry environment, free water in large capillaries will evaporate and diffuse to the outside. This can induce water absorption and interlayer water evaporation to drier capillaries. When absorbed water and interlayer water are moving to capillaries, the thin layers of gel move closer. This leads to concrete shrinkage and deformation. Therefore, plastic shrinkage always accompanies dry shrinkage.

Because of these shrinkage mechanisms, there will be dry shrinkage for cement products made with general water/cement ratio and normal-temperature curing. This study used different materials and techniques, including the use of silica-rich materials, such as RHA, silica fume, etc., superplasticizer, lower water/cement ratios and replacement of part of cement with pozzolanic materials. In order to evaluate the difference in volumes between normal-temperature curing and steam curing, two categories of samples were used. One was made with normal-temperature (25 °C) curing; the others were made with steam curing (65–180 °C). For the normal-temperature group, samples were

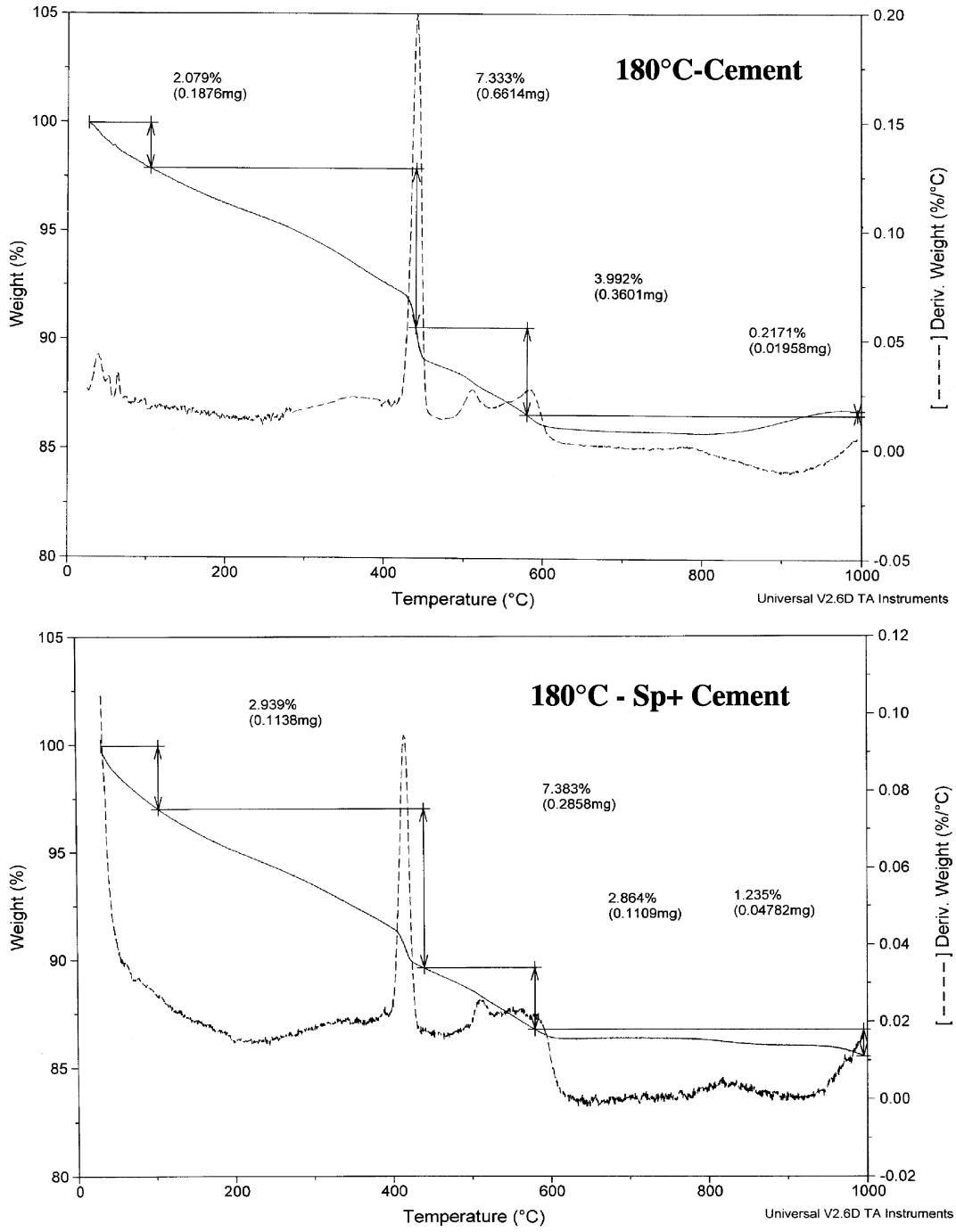

Fig. 6. TGA test data for hydrates in wet-mixed specimens steamed at different temperatures.

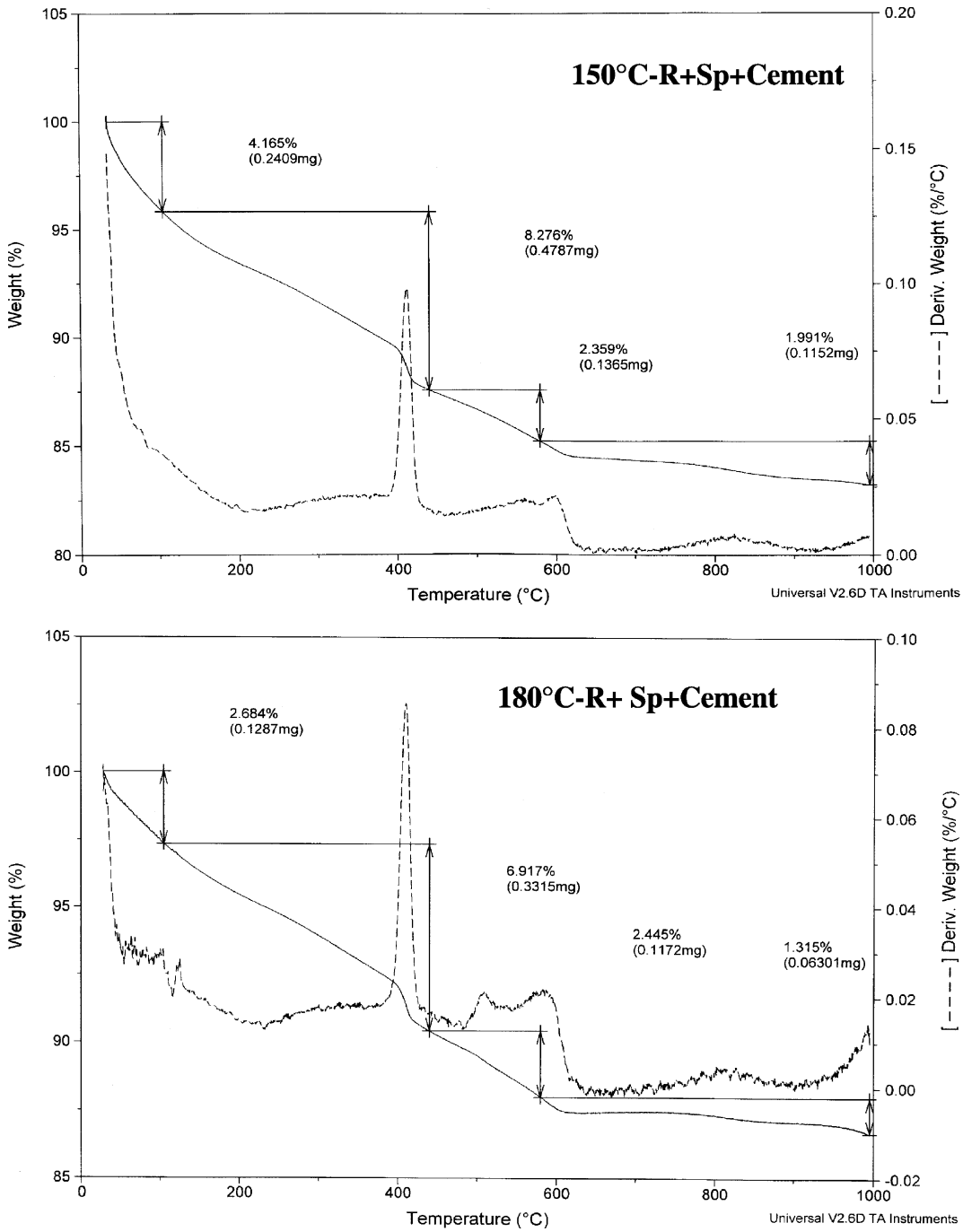

Fig. 6 (*continued*).

removed from the cast 24 h after mixing and then placed in saturated lime solution to cure for 28 days. Then, the length of the sample was measured and taken as the initial length. For the steam curing group, the length of the sample was measured as soon as it cooled down, following steam curing. This length was taken as the initial length for the steam curing group. Both normal-temperature and steam curing samples were placed in a constant-temperature chamber, where the temperature was set at 25 °C. The lengths were measured after 3, 7, 14 and 28 days. Fig. 5 shows the experimental results. In normal-temperature curing, shrinkage of cement with silica-rich materials was less than that of pure cement with the same W/b ratio. The amount of shrinkage was proportional to the amount of cement or water. This result was similar to that reported in the literature where the degree of shrinkage increased with the amount of water or cement. In steam curing, when the curing temperature was under 80 °C, the shrinkage rate with the addition of RHA prepared at 700 °C (R7) was larger than that with the addition of RHA prepared at 850 °C (R8).

This was due to the loose structure of 700 °C RHA, incomplete transformation into silica and higher amount of carbon. When the curing temperature was 120 °C, the sample slightly shrank in early stages. The volume then increased after 28 days, with only slight change in length. When the curing temperature was over 150 °C, all samples were swollen; the higher the temperature, the greater the swelling. This was similar to the condition for below −120 °C curing temperatures. The smaller shrinkage in steam curing and the volume increase with curing temperature were due to the different steam curing mechanisms and the products and pore structures at different curing temperature. With regard to the curing mechanisms, although the retention time were the same, longer curing time was required for higher curing temperatures at the same temperature rate (0.5 °C/min). The total heat energy will increase with the temperature. Therefore, the curing mechanism was different at different curing temperatures. As to the pore structure and water content in the products, it can be found from SEM and TGA experiments that WMSI-processed specimens have less CH (see Fig. 6) and smaller holes and cracks. The smaller amounts of CH, smaller volume and lighter weight of the products indicated that autogenous shrinkage was significant in steam curing. When the curing temperature was over 110 °C, steam should be released for a cool-down rate of 0.5 °C/min after a steam curing process. The autoclave became drier due to lack of steam. This dry environment made the relative humidity (RH) of the samples decrease. It also decreased the potential for shrinkage. Therefore, there was more autogenous shrinkage and less drying shrinkage. Based on the capillary tension theory, surface tension is larger for water in smaller pores. Such water is not easily lost in a dry environment. When water in small pores is lost, negative pressure is larger. In normal-temperature curing, the volumes of CH and AFt were larger than that of tobermorite. The volumes of these CH and AFt can increase; thus, it can inhibit paste shrinkage. Tobermorite, which was not prone to shrink and potential change, was the main product in steam curing, when the amounts of CH and AFt were smaller. This may be due to more autogenous shrinkage in a steam curing process. For this study, the initial length for a steam curing sample was measured when the sample cooled. In this stage, autogenous shrinkage was complete and dry shrinkage was limited. This was contrary to normal-temperature curing. After the initial length was measured, autogenous and dry shrinkage occurred simultaneously for samples in normal-temperature curing. Therefore, the change in length was lower for steam curing samples. When the steam curing temperature was over 105 °C, free water in samples dissipated. Even adsorbed water and interlayer water accompanying free water also dissipated. Therefore, samples were in a dry status. When samples were stored in a 25 °C, 90% RH chamber, they gradually absorbed CO_2 and H_2O in the air. CO_2 can increase the volume of cement products and H_2O can react with CaO in the samples to regenerate $Ca(OH)_2$. These mechanisms may be the main reason for the volume increase in samples prepared at 150 °C curing temperature.

3.4. Effect of curing temperature on compressive strength

As pointed out in the paper [16] (curing temperatures of 13–49 °C), although raising the temperature may increase hydration rates early on, quick hydration may cause higher gel/space ratios on cement surfaces and lower gel/space ratios away from them. In this research, we had the condition during low-temperature curing. Since concrete is a composite material, the strength of concrete depends on the overall strength of its composition. For high-temperature curing, dense hydration products quickly form on the surface of cement. The diffusion time is not long enough for cement to diffuse evenly. Therefore, hydration products do not distribute uniformly in gel space. This leads to a strength lower than those obtained at normal curing temperature. This study also found the same result under lower-temperature steam curing (80 °C). However, when the steam curing temperature is over 150 °C, the deficiencies with low-temperature curing are improved, as stated below.

3.4.1. Comparison of WMSI time

In this experiment, we used RHA pastes with different CaO/SiO_2 ratios and WMSI treated them at 180 °C. The results are shown in Fig. 7. The compressive strengths of the specimens with RHA vary with the CaO/SiO_2 ratio and the retention time. If the retention time is more than 8 h, the specimens would be close to the terminal crystallization stage. The products from the early hydration stages approach steady state. Heat energy from WMSI contributes less to the reaction of the specimens under this circumstance. For any CaO/SiO_2 ratio, one is less affected by the ratio than those that have settled for 2–4 h. This causes the compressive strength to be below 100 MPa, with the worse ones around 80 MPa. In the group with 2-h retention time, the compressive strength is more stable in the group that has an 8-h WMSI delay. It is also not affected by the CaO/SiO_2 ratio (about 90 MPa). With the same delay, the compressive strengths of the rest of the group (all below 85 MPa) are all worth than the compressive strengths of those groups with $\geq$4 h of holding; this is due to the fact that newly mixed pastes are still in their early formation stages in the first 2 h. There is more loose water in the pastes. When WMSI is at high temperatures, the loose water boils, damaging the bonds of the products, causing cracks in specimens and weakening their compressive strengths. In the group with 4-h retention time, the best ones are those with an 8-h delay before WMSI, regardless of the CaO/SiO_2 ratio. The compressive strengths are proportional to the CaO/SiO_2 ratio, i.e., $CaO/SiO_2 = 2.0$ group has 20% more strength than the $CaO/SiO_2 = 1.5$ group does. Results from WMSI at low temperatures are not quite the same as those from high-temperature WMSI, as shown in Fig. 8. For the same materials and retention conditions, 12-h WMSI is slightly better than 8-h one. However, the extra 4 h of WMSI

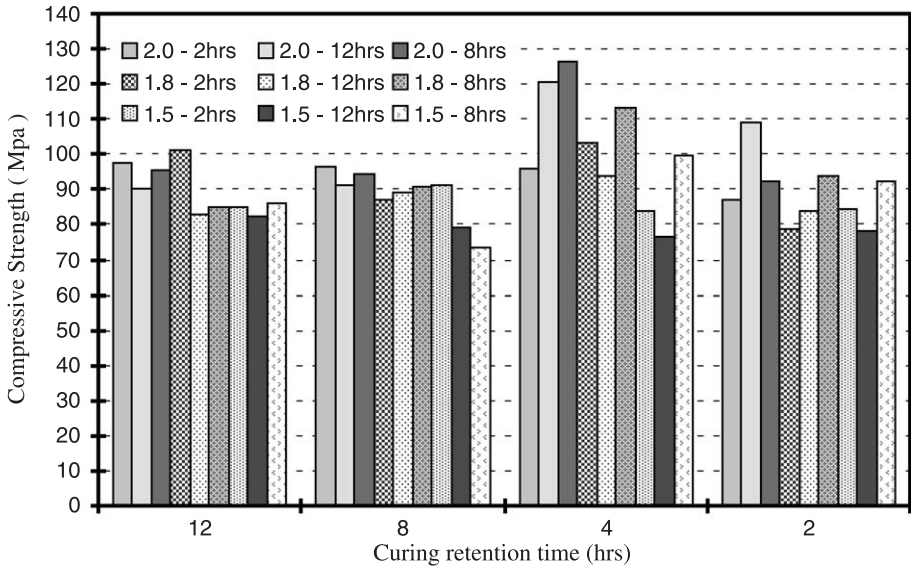

Fig. 7. Compressive strengths of wet-mixed specimens steamed at different curing retention time (180 °C RHA, C/S = 1.5, 1.8 and 2.0, presteaming period = 2, 8 and 12 h).

and energy only increase the strength by 2–4%. It remains to be evaluated whether this is economical.

3.4.2. Comparison of WMSI temperatures

The 65–80 °C group has an increased heating rate during WMSI (0.5 °C/min) as temperature increases. The total kinetic heat energy also increases. In theory, the hydration reaction should accelerate. However, the final compressive strength is related to the retention time before WMSI and the degree of crystallization of a paste in a heating process (subject to the effects of the mixing ratio, amount of water used and retention ambient temperatures).When high-temperature WMSI is used, if the retention and delay times are the same as those of low-temperature WMSI and the heating and cooling rates are both set at 0.5 °C/min, the higher the temperature, the longer the heating and cooling times are, before and after the WMSI delay (8 h). (For example, the heating and cooling times at 180 °C are both 7.6 h longer than those at 65 °C). This means that high temperatures cause some crystals formed at low temperatures to stabilize as a result of longer WMSI. They may also become another product, even the types that can only be produced at high temperatures. Based on the previously mentioned temperatures and WMSI maturity, the 80 °C group should be better than the 65 °C. However, Fig. 8 does not show clear experimental results. Fig. 9 uses a 1.8 CaO/SiO_2 ratio. With a 4-h retention time, it is found that the compressive strengths are different if different materials and WMSI temperatures are used. If the same materials are compared, the higher the WMSI temperature, the higher the compressive strength. For

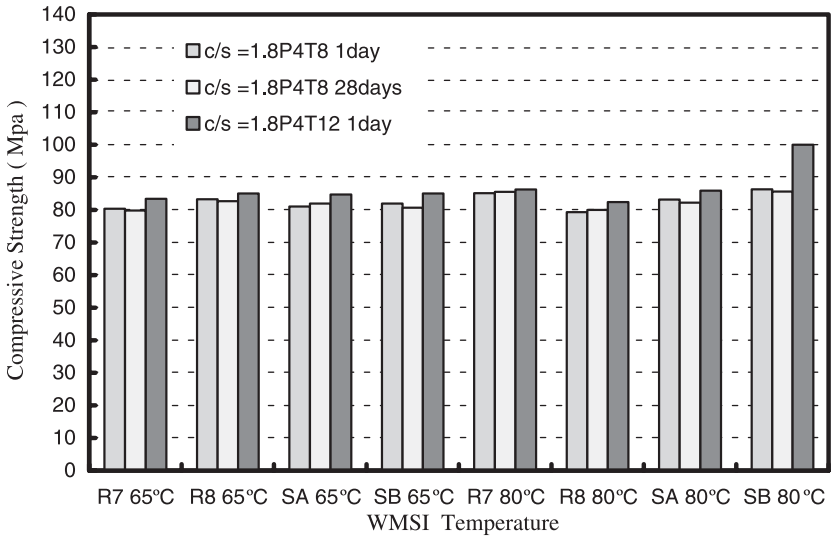

Fig. 8. Compressive strengths of wet-mixed specimens steamed at low temperatures for different delay times.

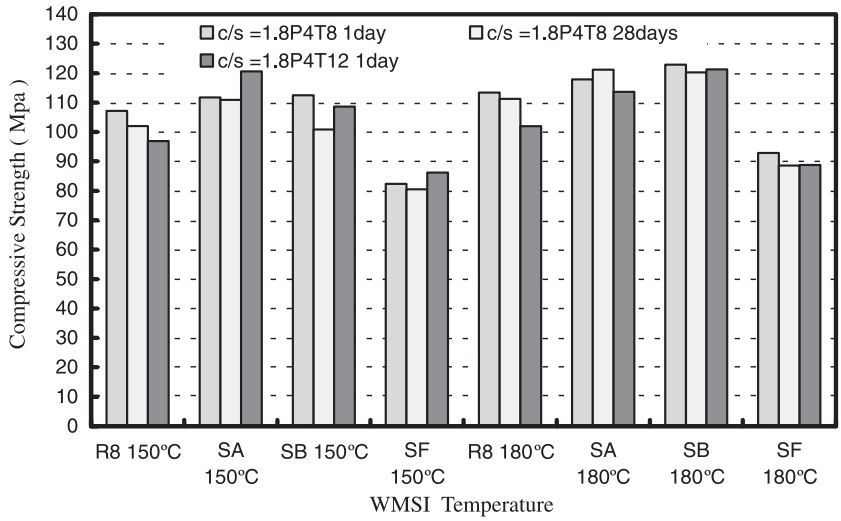

Fig. 9. Compressive strengths of wet-mixed specimens steamed at high temperatures for different delay times and ages.

the same curing temperature, compressive strength is in the following order: fine silica sand>coarse silica sand>850 °C RHA>700 °C RHA>silica fume, which means that, in terms of the compressive strength, the silica sand group is better than the other two types of silica-rich materials. Fine ones are better than coarse ones. However, this is different from the literature [7]. The literature shows that finer silica sand can produce tobermorite earlier, but the maturity is worse in the late phase. It also indicates that the coarser the silica sand, the better the tobermorite crystal and the better the compressive strength of Yang's module. The difference is due to the fact that the diameters of silica sand (0.3 and 0.15 mm) in this study were larger than those (4.3–32.3 μm) used in the literature. There should be an optimal diameter range of silica sand for high-temperature steam curing. If the diameter is over or under this range, it cannot be beneficial to the strength characteristic.

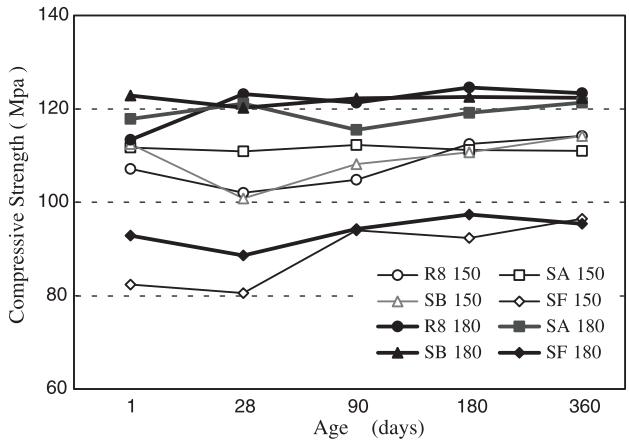

Fig. 10. Compressive strengths of wet-mixed specimens steamed at high temperatures for different curing times in water.

3.4.3. Comparison of different storage times after curing

Ref. [16] indicates that higher steam curing temperatures (12.8–48.9 °C) can increase the hydration rate. The compressive strength of 1-day samples increases with the curing temperature. However, at 28 days of age, the strength is lower for samples that showed higher strength in the early phase. For this study, the pastes were quiescent for 4 h, heated up at 0.5 °C/min after each was WMSI treated at 65–180 °C for 8 h. Then, they were cooled down to the normal temperature and stored in a 25 °C saturated limewater for 28 days. The results showed that most experimental groups at age 28 days have 1–3% lower compressive strengths than they do at 1 day of age, consistent with the conclusions of Ref. [16]. If they are cured for a year, then their compressive strengths are close to or higher than those at 1 day of age, as shown in Fig. 10. This means that WMSI-treated pastes will have slightly lower compressive strengths in 1–3 months and slowly increasing compressive strengths later as they age.

4. Conclusions

1. High-temperature steam curing generates more products than low-temperature steam curing and contributes more to the strength. If low-temperature curing is used, then the temperature should be lower than 65 °C and the curing retention time should be more than 12 h in order to obtain a higher quality than that obtained from normal-temperature curing.
2. At normal temperatures, adding RHA and silica is better due to the pozzolanic reaction. However, adding silica sand is not better. Steam injection at 65–120 °C does not significantly increase the compressive strength. The shortened period for crystal formation causes the structure of the matrix to be inferior to that obtained

with 28-day, normal-temperature curing. If the steam injection temperature is above 150 °C (180 °C is even better), on the surface of silica sand, $C_2S_3H_X$ is generated in silica-rich layers, which will increase the compressive strength to a level higher than that of the RHA and silica group.

3. In the initial stage of normal-temperature curing, strength is provided by C_3S. In later stages, strength is supplemented by C_2S. After high-temperature steam injection, the degrees of hydration of C_3S and C_2S are 85% and 45%, respectively. (In the RHA group, they are 90% and 60%, respectively.) Immersing the specimen in 25 °C limewater for 28 days of curing does not increase the degree of hydration. This means that high-temperature steam injection can only cause C_2S in cement to generate 50% hydration. The total amount of shrinkage is less than that of normal-temperature curing. When silica-rich materials are used, we may increase C_3S in cement and decrease C_2S to improve the results.

1 lb	0.454 kg
1 kis	6.895 MPa
CSH	CSH gel
Sp	superplasticizer
SF	silica fume
C	CaO
S	SiO_2
R7	700 °C RHA
R8	850 °C RHA
1.8 P4 T8	$CaO/SiO_2 = 1.8$, presteaming period 4h, curing retention time 8 h
1 in	2.54 cm
CH	$Ca(OH)_2$
Psi	bonding lengths of CSH gel polysilicate anion
α	degree of hydration
SA	ASTM C109 sand
SB	ASTM C190 sand

Acknowledgements

The authors thank the National Science Council of the Republic of China for the financial support (grant nos. NSC87-0410-E-009-043 and 85-0410-E-009-016) that made this publication possible.

References

[1] S. Mindess, J.F. Young, Concrete, Prentice-Hall, Englewood Cliff, NJ, 1981.
[2] W.M. Lin, T.D. Lin, C.L. Hwang, Y.N. Peng, Fundamental study on hydration of cement and cement minerals with steam, ACI Mater. J. 95 (1) (1998) 37–49.
[3] U.Z. Hwang, Investigation on the strength loss and methods of strengthening for autoclave concrete, Master's degree thesis, Dept. Civil Eng. Natl. Chung Hsing Univ., Taiwan, 1995, pp. 63–69.
[4] ACI Committee 517, Accelerated curing of concrete at atmospheric pressure, Revised version, ACI Detroit, MI, 1992.
[5] ACI Committee 516, High pressure steam curing modern practice and properties of autoclave products, ACI Mater. J. 62 (8) (1962) 869–908.
[6] F.M. Lea, The Chemistry of Cement and Concrete, Edward Arnold, London, 1980, pp. 185–203.
[7] N. Isu, H. Ishida, T. Mitsuda, Influence of quartz particle size on the chemical and mechanical properties of autoclaved aerated concrete (I) tobermorite formation and (II) fracture toughness, strength and micropore, Cem. Concr. Res. 25 (2) (1995) 243–254.
[8] J.Y.R. Yen, Strength development and associated micro structure change of autoclaved concrete, The 19th Conference on Our World in Concrete and Structure, Conference Documentation Vol XIII, C1-Premier Pte Ltd, Singapore, 1994, pp. 231–237.
[9] T. Mistuda, K. Sasaki, H. Ishida, Phase evolution during autoclaving process of aerated concrete, J. Am. Ceram. Soc. 75 (7) (1992) 1858–1863.
[10] Y.N. Peng, R.H. Weng, J.C. Yan, Mechanic properties of different fineness slag-cement paste with DMSI, The 3th National Conference on Structural Engineering, Chinese Institute of Civil and Hydraulic Engineering, Taiwan, 1996, pp. 749–758.
[11] Y.N. Peng, R.H. Weng, J.Y. Huang, Mechanic properties of fly ash cement paste with DMSI, The 3th National Conference on Structural Engineering, Chinese Institute of Civil and Hydraulic Engineering, Taiwan, 1996, pp. 847–856.
[12] Y.N. Peng, M.C. Zaw, D.S. Wu, Mechanic properties of transition zone of slag-cement paste/aggregate through DMSI process, The 4th National Conference on Structural Engineering, Chinese Institute of Civil and Hydraulic Engineering, Taiwan, 1998, pp. 181–188.
[13] D.S. Wu, Chemical and Physics Analysis of Rice Husk Ash and the Effect of Best Combustion Condition on Cement Hydration, Chung-Te, Taiwan, 1989.
[14] P.K. Mehta, Portlanic and cementitious by products as mineral admixture—a critical review, First International Conference on Use of Fly Ash, Silica Fume, Slag and Other Mineral By-Products in Concrete, ACI SP-79, American Concrete Institute, Canada, 1983, pp. 1–46.
[15] G. Verbeck, L.E. Copeland, Some physical and chemistry aspects of high pressure steam curing, Paper SP.32-I, PC 4-2-2-5, PCA, USA.
[16] C.A. Menzel, High pressure stream curing, ACI SP-32, Detroit, 1972.
[17] H. Justnes, I. Meland, J.O. Bjoergum, J. Krane, T. Skjetne, NMR a powerful tool in cement and concrete research, SINTEF Rapp. (1989) 1–22.
[18] A.M. Neville, Properties of Concrete, Pitman, London, 1981, p. 374.